Oxidative degradation of Rhodamine B in aqueous solution using Fe/PANI nanoparticles in the presence of AQS serving as an electron shuttle

Xinxin Yue, Zhonghua Liu, Qiying Zhang, Xianghui Li, Feifei Hao, Jing Wei, Weilin Guo*

School of Resources and Environment, University of Jinan, Jinan 250022, China, emails: 956299257@qq.com (X. Yue), 1570938820@qq.com (Z. Liu), 444154402@qq.com (Q. Zhang), 18766106007@163.com (X. Li), ljffyjs09@163.com (F. Hao), stu_weij@ujn.edu.cn (J. Wei), Tel./Fax: +86 531 8276 9233; email: chm_guowl@ujn.edu.cn (W. Guo)

ABSTRACT

In this study, core-shell Fe^0@polyaniline (PANI) nanoparticles were synthesized to remove Rhodamine B (RhB) in aqueous solution. The Fe^0/PANI composites were characterized by X-ray diffraction, Fourier transform infrared spectra, and transmission electron microscopy. The performances of Fe^0/PANI on the activation of molecular oxygen for the removal of RhB were investigated, and the effects of operating parameters, such as Fe^0/PANI dosage, RhB initial concentration, and pH value on RhB removal were also discussed. The results indicated that the Fe^0@PANI/O_2 process exhibited significantly higher reactivity than did the Fe^0/O_2 process for the degradation of RhB. The oxidative degradation of RhB was further promoted by the presence of anthraquinone-2-sulfonic acid sodium salt working as an electron shuttle. In addition, the reaction mechanism was discussed by measuring the concentrations of Fe(II), and total Fe formed in the system and examining scavenging effect by tert-butyl alcohol and copper chloride. The redox mediating function of PANI was also revealed by the UV–vis spectra. The stability of Fe^0@PANI showed that it is a potential nanomaterial for the environmental remediation.

Keywords: Core-shell Fe^0@PANI nanoparticles; Dioxygen activation; Rhodamine B; Electron shuttle; Anthraquinone-2-sulfonic acid sodium salt; Degradation

1. Introduction

Iron is a low-cost, naturally abundant, and environmentally friendly material that has been widely applied in remediation of various contaminants in water or soil [1]. Nano zero-valent iron (nZVI) has the remarkable capability to degrade organic materials and to adsorb inorganic contaminants, and it showed great potential for environmental remediation of contaminants in soils, sediments, and groundwater [2]. Compared with commercial iron powders, the nZVI materials have many advantages, such as larger surface area and higher reactivity. The nZVI-Fenton process was regarded as a very effective process for the treatment of hazardous, refractory, and non-biodegradable organic pollutants in various types of wastewater [3].

Although nZVI shows the desirable properties such as high dehalogenation activity and injectability into deep and overbuilt aquifers, it also shows

*Corresponding author.

undesirable properties such as a pronounced agglomeration tendency, untimely deposition, blocking of flow paths and hence a very limited mobility under aquifer conditions [4]. Agglomeration can significantly decrease the effective surface area of nanoparticles and thus reduces their catalyst performance. The stability of iron nanoparticles against aggregation can be improved by imparting electrostatic repulsion, applying organic surfactants, or by utilizing capping agents or supporting inorganic material [5]. For example, nZVI coated with SiO_2 have been proved to show good property for elimination of polybrominated diphenyl ethers [6]. The SiO_2@FeOOH@Fe nanoparticles were shown to have higher reusability and stability, as they could be reused more than seven times, and that the SiO_2@FeOOH@Fe can effectively avoid leaching iron ions into the solution and causing secondary pollution in the reaction. An Fe-activated carbon composite which consists of nanoscale zerovalent iron clusters on activated carbon colloids is especially designed for the *in situ* generation of reactive zones and contaminant source removal when applied in groundwater remediation processes [7,8].

Significant scientific effort has been directed at investigations of conducting polymers as composite components. Conducting polymers can be used as suitable host matrices for dispersing catalyst particles. Conducting polymer/catalyst nanoparticles permit a facile flow of electronic charges through the polymer matrix during the electrochemical process. In the development of nanocomposites, coating of various substrates with a thin polymer film has been reported [9]. To some extent, surface modification of nZVI by polymers has been shown to rapidly improve the catalytic performance of nZVI. Moreover, the porous structure of the matrix allows high hydraulic conductivity, which is in favor of faster degradation rates in water system [10].

Among conducting polymers, polyaniline (PANI) is the most intensively studied one due to its controllable conductivity, environmental stability, and rather simple synthesis [11]. The introduction of PANI would give new properties into the nanocomposite. A PANI membrane containing iron particles was developed and tested as a model barrier for contaminants [12].

Numerous studies have been reported using PANI/Fe as an adsorbent [13,14], but there are few studies about the oxidative degradation of Rhodamine B (RhB) in aqueous solution using Fe/PANI nanoparticles. In Fenton or photo-Fenton process, O_2 is decomposed to hydroxyl radicals that can easily react with organic compounds in the presence of Fe(II). However, this process is not a very effective means of degrading contaminants because the yields of oxidants are usually low (i.e. typically less than 5% of the iron added is converted into oxidants capable of transforming organic compounds) [15].

During the last two decades, the catalytic effects of different redox mediators on the degradation processes of pollutants have been studied, which include humic acid (HA), antraquinone-2,6-disulfonate (AQDS), polyformaldehyde (POM), hydroquinone, and some aromatic compounds [16,17]. Evidence has been accumulated that HAs, and particularly their quinonoid moieties, can play an important role as redox mediators in different metabolic pathways [16]. And the HA analog AQDS can also serve as an electron donor in the microbial reductive dechlorination of TCE to cis-DCE [17]. The addition of polyoxometalate greatly increases the yield of oxidants in the $nZVI/O_2$ and the $Fe(II)/O_2$ systems [15]. Under acidic conditions, POM mediates the electron transfer from nZVI or Fe(II) to oxygen, increasing the production of hydrogen peroxide, which is subsequently converted to hydroxyl radicals through the Fenton reaction. Polyhydroquinone is also a redox-active polymer with quinone/hydroquinone redox active units in the main chain. The influence of polyhydroquinone in the Fe_3O_4/persulfate system was examined [18].

This study aims to understand the degradation of RhB in aqueous solution utilizing core-shell Fe^0@PANI nanoparticles which is further promoted by the presence of anthraquinone-2-sulfonic acid sodium salt (AQS) working as an electron shuttle. The effects of the key parameters including catalyst dosage, pH value, and initial RhB concentration on the RhB removal were examined.

2. Experimental

2.1. Chemicals and materials

RhB (Analytical grade) was obtained from Shanghai Chemical Reagent Co. Ltd (Shanghai, China). All the other chemicals were of analytical grade and were provided from Tianjin, China, including $FeSO_4 \cdot 7H_2O$, $NaBH_4$ (96%), aniline, ethanol, copper chloride, N, N-dimethylformamide (DMF), tert-butyl alcohol (TBA), AQS, ammonium persulphate (APS), and 4-Methylbenzenesulfonic acid (MBSA). The water used in all experiments was purified by a Milli-Q system and deoxygenated prior to reaction by bubbling nitrogen gas for 1 h.

2.2. Preparation and characterization of core-shell Fe^0@PANI

nZVI was successfully synthesized using reduction process of ferric nitrate solution with sodium

borohydride following the process. The preparation was carried out in a 500-mL flask attached to a vacuum pump. First, 0.02 mol FeSO₄·7H₂O was dissolved into 100 mL ethanol solution (30% volume) with vigorous agitation. After sparging with N_2 for 15 min, 100 mL, 0.01 mol/L borohydride solution was slowly added into the above mixture and stirred for 20 min at 25°C. Fe^{2+} was reduced by BH_4^- to form black nZVI particles immediately. nZVI particles were collected by vacuum filtration and washed several times with deionized water and ethanol. The resulting black solids were vacuum dried for 10 h at 40°C, broken up by a spatula and stored in a N_2-purged desiccator. The final products were dried and stored in a vacuum drier [19].

PANI was prepared as described previously with some modification [20]. Specifically, aniline (5 mL) and MBSA (5.0 g) were dissolved in two different 40 mL deionized water, respectively. The aniline and MASA solutions were rapidly mixed and stirred in conical flask under the nitrogen atmosphere. Then 20 mL solution of APS (12.5 g) was added drop by drop into the mixture at the speed of 1–2 drops per second and stirred vigorously and continuously under nitrogen atmosphere in an ice bath. Once all of the APS solution was added, the mixture was stirred continuously in an ice bath for 6 h. The precipitates were filtered and washed with deionized water and then with acetone, dried at 60°C in vacuum drying oven for 24 h, and finally ground into fine powder.

PANI and iron particles were mixed in a small amount of DMF and then dry the mixture in vacuum at 70°C for 6 h. The dried sample was kept in inert atmosphere. The PANI/nZVI composites were prepared with a PANI/nZVI mass ratio of 1:10.

A black powder was obtained and characterized by the following techniques. X-ray diffraction (XRD) patterns were recorded on a Philips X'Pert Pro Super X-ray diffractometer with a Cu Kα source ($\lambda = 1.54178$ A). Fourier transform infrared (FTIR) spectra were recorded on a Bruker VERTX-70 FTIR spectrometer using KBr pellets containing 1% weight sample. It was determined in the frequency range 400–4,000 cm^{-1} with a resolution of 4 cm^{-1}.

2.3. Batch oxidation experiments

Stock solution of RhB (0.8 mmol/L) was prepared using deionized water. The degradation experiments were conducted in 500-mL beaker flasks. Flasks were prepared in duplicates for all experiments. The reaction was initiated immediately by adding 10 mL of aqueous RhB solution, 20 mg Fe⁰@PANI, and an appropriate dosage of AQS. Degradation experiments were carried out under continuous magnetic stirring

at room temperature. At given intervals, 5 mL of the suspension were extracted from each flask and subsequently centrifuged at 8,000 rpm for 1 min with a TGL-16C centrifugal (Shanghai, China) to eliminate the sample powders. The concentrations of the residual RhB were determined by monitoring the decrease in absorbance at the maximum wavelength (554 nm) with UV–vis spectroscopy.

The effect of oxygen was investigated in which the reaction solution was sparged with air or N_2 for 1 h prior to reaction initiation. Furthermore, dominating reactive radicals responsible for the degradation process were identified by quenching studies using two kinds of reagents, viz. TBA and copper(II), with markedly different reactivities toward hydroxyl radicals and superoxide anion. The concentrations of Fe(II), Fe(III), and total iron formed in the process were measured according to a 1,10-phenanthroline spectrophotometric method.

For the recycle runs of RhB degradation, the used catalyst was collected by centrifugation, washed with deionized water and ethanol, and dried in vacuum oven at 50°C for 12 h. Owing to the small particle sizes, catalyst loss was unavoidable in the process of washing and drying. Thus, several parallel reactions were conducted in the four runs to ensure that the dose of recycled catalyst was sufficient for the next run. Catalyst dose and other reaction conditions remained the same for the subsequent runs.

3. Results and discussion

3.1. Characterization of Fe⁰@PANI

The XRD pattern of Fe⁰@PANI was investigated. The characteristic peak at $2\theta = 44°–45°$ assigned to Fe⁰ (α-Fe) confirmed the presence of zero-valent iron in freshly prepared Fe⁰@PANI as depicted in Fig. 1, where no characteristic peaks of ferric oxide were observed, suggesting the non-oxidation of nZVI [21,22]. The average particle sizes of nZVI calculated from the Scherer formula are about 52.7 nm.

The FTIR spectra of Fe⁰@PANI and PANI were shown in Fig. 2. Broad and strong peaks at about 3,400 cm^{-1} (OH stretching vibration) and peaks at 1,630 cm^{-1} (OH bending vibration) indicated the presence of physisorbed interstitial water molecules on the surface of nZVI [23]. The peaks at 1,632 cm^{-1} correspond to the C=N stretching vibrations of quinoid rings of PANI. Peaks at 1,384 and 1,120 cm^{-1} are due to the stretching mode for the benzenoid ring and the peak at about 800 cm^{-1} can be ascribed to out of plane bending of C–H [24]. The characteristic peaks of PANI can be found from the spectrum of the Fe⁰@PANI
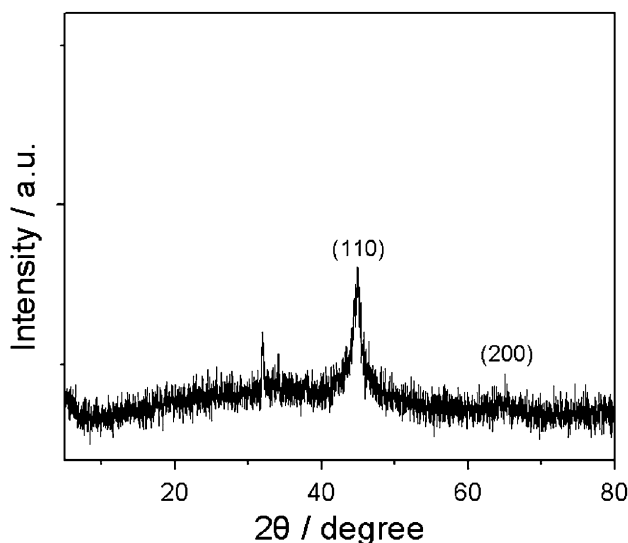
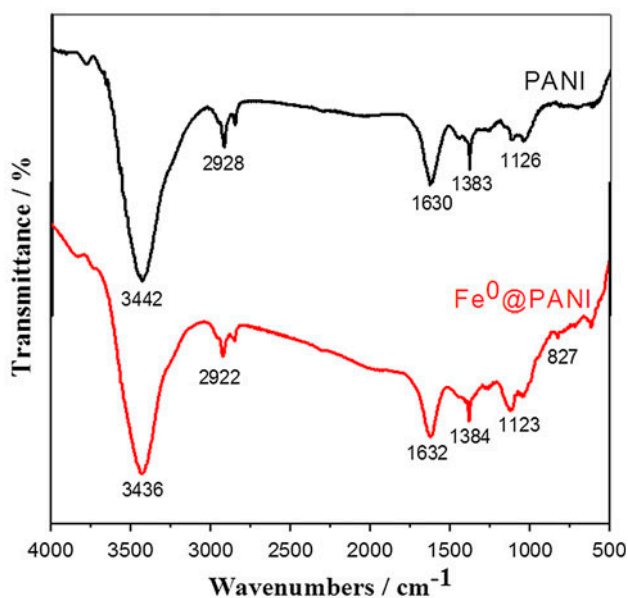Fig. 1. XRD pattern of Fe^0@PANI nanoparticles.

Fig. 2. FTIR spectra of PANI and Fe^0@PANI nanoparticles.

composite that are in agreement with similar data reported in the literature [25], which indicated that nZVI was coated by PANI.

The TEM images of Fe^0@PANI show that the Fe^0@PANI particles were nearly spherical with a size range of 30–90 nm in diameter, and these nanoparticles have a core-shell structure (Fig. 3). The shell (about 4.2 nm) probably resulted from PANI, while the core was attributed to Fe^0 [26]. The aggregated structure of Fe^0 particles was attributed to the magnetic forces and van der Waals forces between Fe particles.

3.2. Effect of operational parameters on the degradation of RhB

RhB was chosen as representative organic compounds in this study. The reactivity of four samples was evaluated by the aerobic degradation of RhB at room temperature (Fig. 6). 7.5% of RhB was removed over PANI in 2 h, while higher efficiencies of 46.8, 60.1, and 90.1% for Fe^0, Fe^0@PANI, and Fe^0@PANI/AQS were observed. The results showed that Fe^0@PANI is an efficient catalyst for oxidation elimination of RhB in the presence of O$_2$, and the introduction of AQS greatly enhanced the dioxygen activation and catalytic degradation of RhB.

As shown in Fig. 4, little removal of RhB (about 7.5%) occurs when adding into the solution with PANI only, indicating the effect of adsorption on RhB removal is not obvious. O$_2$ can be activated by nZVI to generate reactive oxygen species (ROS), which can effectively oxidize RhB in solution. However, this process is not a very effective means of degrading contaminants because the yields of oxidants are usually low and nZVI materials have a strong tendency to agglomerate which can significantly decrease the effective surface area of nanoparticles and thus reduces their catalyst performance. Therefore, the composite with surface modification of nZVI by PANI presented smaller particle size, and exhibited higher reduction reactivity because of more accessible surface [27]. The degradation of RhB follows the pseudo first-order kinetics (ln $c_0/c = 0.022t + 2.101$, $R^2 = 0.9582$).

Several studies confirmed that the quinone-containing compounds serve as an electron mediator to enhance the degradation rate of pollutants in Fenton or photo-Fenton system [28]. Since AQS contains quinine structure, it can act as an electron transfer
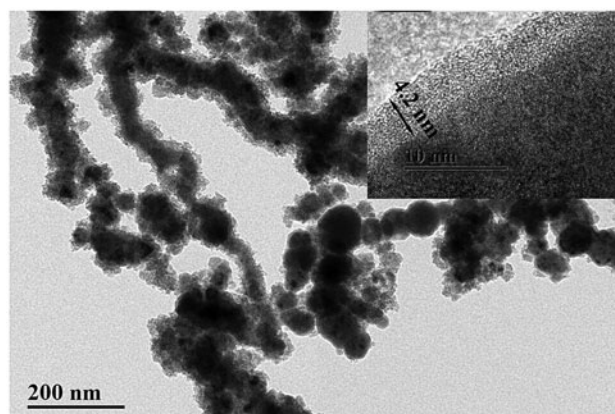

Fig. 3. TEM and HRTEM (inset) images of the core-shell Fe^0@PANI nanoparticles (scale bar in the inset 10 nm).
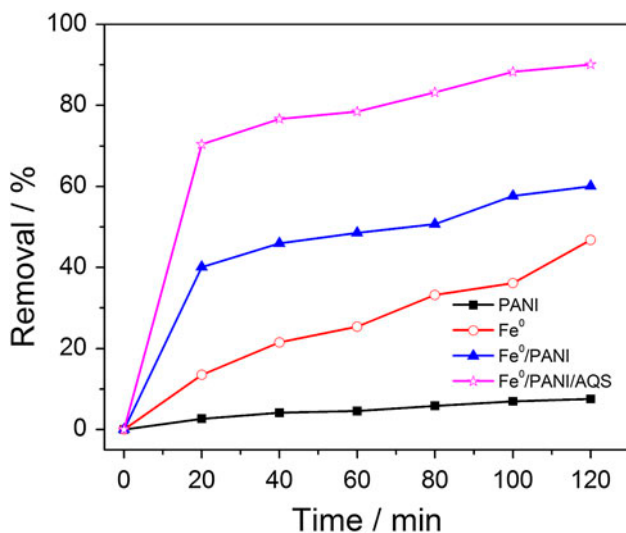
Fig. 4. Degradation curves of RhB under different conditions (Fe^0, 0.018 g; PANI, 0.02 g; Fe^0@PANI, 0.02 g; AQS, 100 mg/L; initial concentration of RhB, 0.005 mmol/L; pH 6.57).

Fig. 5. Effect of AQS concentration on the degradation of RhB (Fe^0@PANI, 0.02 g; initial concentration of RhB, 0.005 mmol/L; pH 6.57).

mediator in the Fe^0@PANI/O_2 system, we tested the oxidative degradation of RhB in the presence of AQS. The addition of AQS can markedly enhance the removal efficiency of RhB in the Fe^0@PANI/O_2 system (Fig. 4). It may be because that AQS mediates the electron transfer from nZVI to oxygen, increasing the production of hydrogen peroxide, which is subsequently converted to hydroxyl radicals through the Fenton reaction.

Effects of AQS concentration on the RhB degradation were also investigated and the results are shown in Fig. 5. One can see that the degradation of RhB is strongly affected by the concentration of AQS in aqueous solution. As shown, the increase in the AQS concentration in the solution from 0 to 100 mg/L resulted in almost two fold of the degradation efficiency of RhB; however, a further increase of the AQS concentration to 200 mg/L showed a comparatively smaller improvement in the extent of reaction.

Catalytic properties of Fe^0@PANI composites with different weight ratios of Fe^0 and PANI were determined for oxidative degradation of RhB. As shown in Fig. 6, the catalytic property of the Fe^0@PANI composites decreased as their ratios of Fe^0/PANI decreased, suggesting that these ratios should be considered an important parameter when Fe^0@PANI composites are prepared for RhB treatments. The higher removal efficiency of Fe^0@PANI composite with a ratio of 1:0.1 largely attributes to the oxidative degradation ability of nZVI and the adsorption capacity of PANI. However, the lower percentage of PANI in Fe^0@PANI

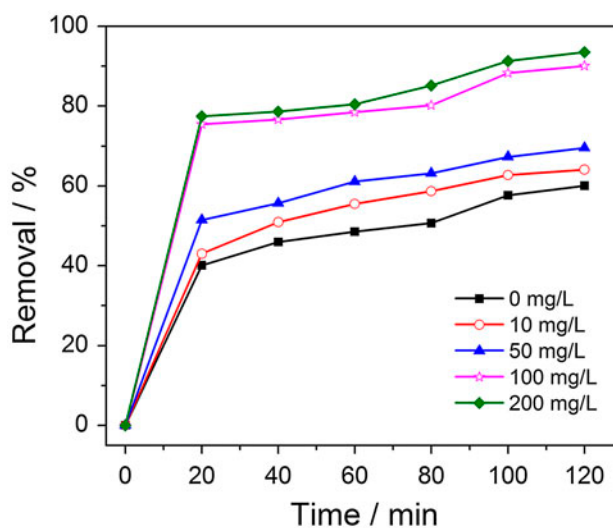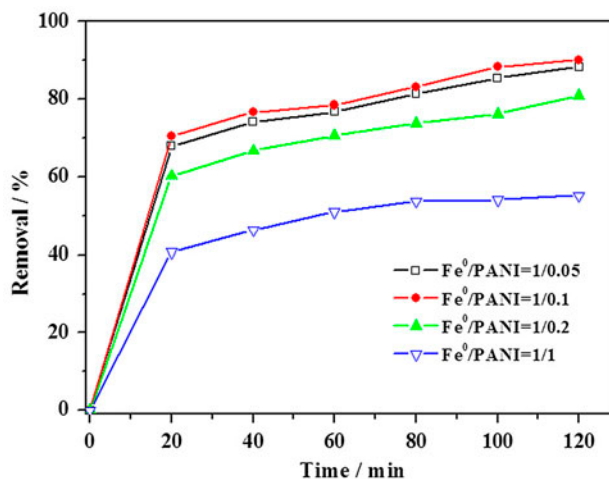Fig. 6. Effect of Fe^0@PANI composites with different weight ratios of Fe and PANI on the degradation of RhB (Fe^0@PANI, 0.02 g; initial concentration of RhB, 0.005 mmol/L; AQS, 100 mg/L; pH 6.57).

composite with a ratio of 1:0.05 easily leads to the aggregation of the nZVI [4], impeding the oxidative degradation ability of nZVI. With increasing the amount of PANI, the surface pore size of PANI decreases, therefore it becomes more and more difficult for O_2 to get through the mesoporous, consequently the degradation of RhB decreased.

For checking the catalytic activity of Fe^0@PANI on the degradation of RhB, one set of experiments was conducted by varying the concentrations of RhB. Fig. 7 presented that the removal percentage of RhB

decreased from 91.4 to 48.3% with the increase of the initial RhB concentration from 0.0025 to 0.02 mmol/L for 2 h. Owing to the constant amount of Fe^0@PANI, the rate of ROS production remains constant and the effect would be reduced with higher RhB concentration.

It is known that the generation of ROS in the reaction of Fe^0 with O_2 and the subsequent organics oxidation are strongly correlated to the pH of the solution [29]. Therefore, the effect of pH value on the degradation of RhB was also studied, and the results were presented in Fig. 8. In this research, the influence of pH on the degradation of RhB was explored by adjusting the solution pH to 3.25, 4.42, 6.57, 10.33, and 11.38. The reaction was conducted at ambient temperature in the presence of 5 mg/L RhB, 100 mg/L AQS, and 0.02 g Fe^0@PANI.

As can be seen from Fig. 8, pH value made a decisive influence on the removal of RhB in the Fe^0@PANI/O_2 system. 94.9% RhB removal was achieved at pH 3.25, and the removal efficiency of RhB varied in the range of 60.5–90.6% with the initial solution pH further increasing from 4.42 to 11.38. Therefore, it can be concluded that the acidic pH facilitated the removal of RhB. One possible explanation is that H^+ enhances the corrosion of nZVI and promotes the oxidization potential of $\cdot OH$ and $O_2^{\cdot-}$. In the mean time, the degradation of RhB was restrained at the alkaline pH range because OH^- would significantly enhance the formation of the iron hydroxide occupying the reactive sites and thus inhibit the reaction [4]. Moreover, a high pH value may create more
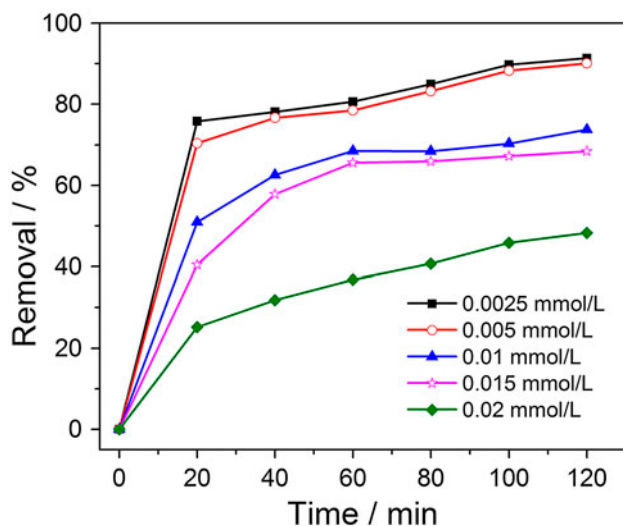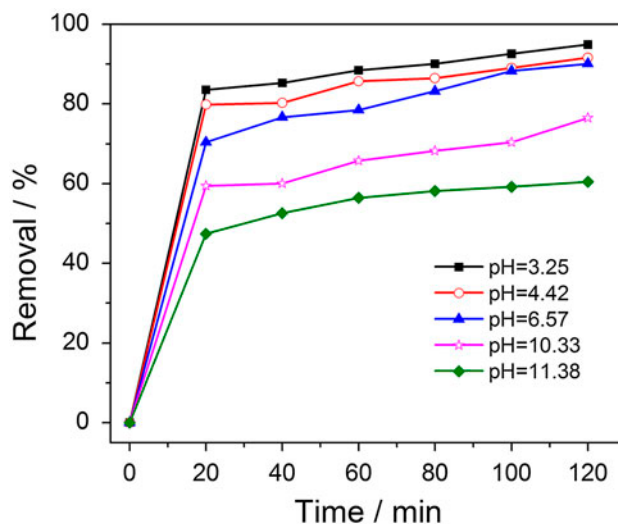

Fig. 8. Effect of pH value on the degradation of RhB (Fe^0@PANI, 0.02 g; AQS, 100 mg/L; initial concentration of RhB, 0.005 mmol/L).

free radical scavengers (i.e. CO_3^{2-}, HCO_3^-) and results in the decrease in the concentration of $\cdot OH$ [30]. These results suggest that under acidic conditions, the Fe^0@PANI/AQS/O_2 system can efficiently degrade RhB in a wide working pH range, which is an important advantage to its application.

As shown in Fig. 9, the removal percentage of RhB increased with various dosages of Fe^0@PANI in the range from 0.005 to 0.04 g. In comparison with the RhB degradation at Fe^0@PANI dosage 0.005 g, there was a remarkable accelerating effect when Fe^0@PANI dosage increased to 0.02 g. However, the degradation efficiency of RhB for a further increase of Fe^0@PANI dosage from 0.02 to 0.04 g showed a comparatively smaller improvement in the extent of reaction. The increase of Fe^0@PANI dosage significantly improved the removal of RhB, which may be due to the faster formation of the active radicals like $\cdot OH$ and $O_2^{\cdot-}$. Considering the practical application and economic cost, 0.02 g Fe^0@PANI was adopted for the further study of the degradation of RhB.

3.3. Proposed reaction mechanism

The active species trapping experiments were then carried out by adding tert-butyl alcohol (TBA, $\cdot OH$ scavenger) and copper chloride (CuCl$_2$, $O_2^{\cdot-}$ scavenger) as scavengers to the aerobic RhB degradation solution in the Fe^0@PANI/O_2 system. It can be seen from Fig. 10 that the 62 and 56% drop in RhB degradation efficiency were observed in the presence of slight CuCl$_2$ and TBA within 2 h, respectively. The addition

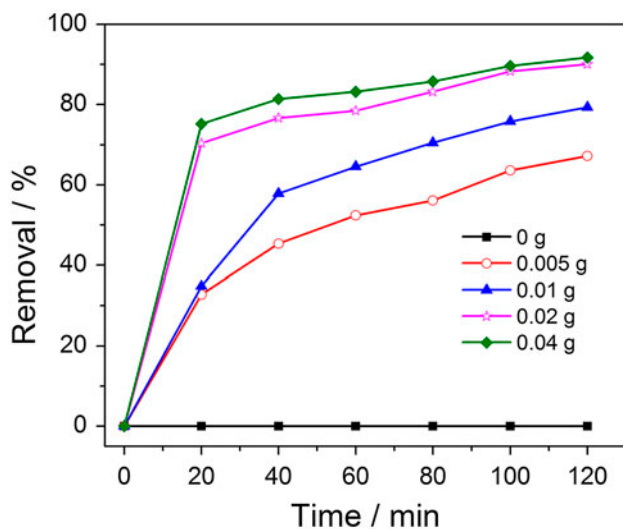Fig. 7. Effect of initial RhB concentration on the degradation of RhB (Fe^0@PANI, 0.02 g; AQS, 100 mg/L; pH 6.57).

Fig. 9. Effect of Fe⁰@PANI dosage on the degradation of RhB (AQS, 100 mg/L; initial concentration of RhB, 0.005 mmol/L; pH 6.57).

of these two scavengers could inhibit the aerobic degradation of RhB, confirming the involving of ·OH and O_2^- species in the aerobic degradation of RhB over Fe⁰@PANI nanoparticles. Compared to the drop of the efficiency of RhB degradation in presence of TBA and CuCl₂, relatively significant drop in presence of N₂ instead of O₂ indicated that ·OH and O_2^- species as oxidizing species was predominantly produced during the activated decomposition of O₂ by Fe⁰@PANI Fig. 11.

The concentrations of Fe(II) and total dissolved irons were quantified by monitoring the absorbance of Fe(II)-orthophenanthroline complex at 510 nm with a UV–vis spectrophotometer [31]. It can be seen from Fig. 12 that the concentration of dissolved Fe(II) increased within 1 h and then unchanged within 2 h, while the total dissolved irons kept increased within 2 h throughout the entire process. As the reaction proceeds, the lattice or sorbed Fe(II) in the surface of Fe⁰@PANI was transformed to Fe₂O₃, which coated on the surface of Fe⁰@PANI and hindered the rate of electron transfer. Therefore, the concentrations of Fe(II) was maintained constant in the solution.

This study proposes a feasible and effective method for activating molecular oxygen to dispose organic pollutants in aqueous solution. It is found that Fe⁰@PANI could be used to transform and mineralize organics in oxygenated water with no need for additional H₂O₂. The reactive oxygen species generated by Fe⁰@PANI in the presence of oxygen plays an important role in the degradation of RhB in aqueous solution [32].

These reactions may occur on or adjacent to the surface of Fe⁰@PANI, which is reactive in water and can serve effectively as an electron donor. First, the contaminant is diffused through the solution to the iron particle surface and adsorbed to a favorable reaction site. Then, electrons are transferred from the core-shell Fe⁰@PANI to the contaminant, producing ferrous ions (Eq. (1)). And it was reported that ferrous ions bound on the surface of iron could activate molecular oxygen via single-electron reduction
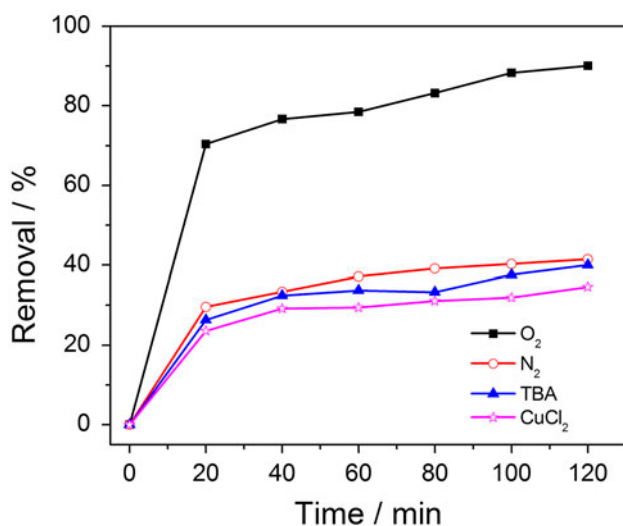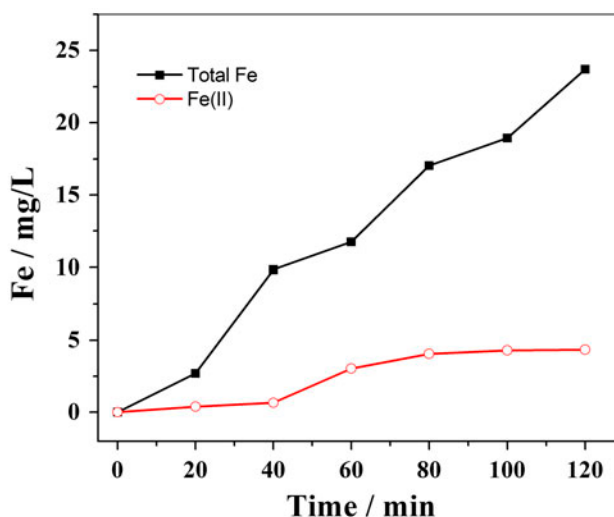

Fig. 10. Comparison of the degradation of RhB under different conditions (Fe⁰@PANI, 0.02 g; AQS, 100 mg/L; initial concentration of RhB, 0.005 mmol/L; pH 6.57).

Fig. 11. The concentrations of Fe(II) and total Fe formed in the degradation of RhB (Fe⁰@PANI, 0.02 g; AQS, 100 mg/L; initial concentration of RhB, 0.005 mmol/L; pH 6.57).
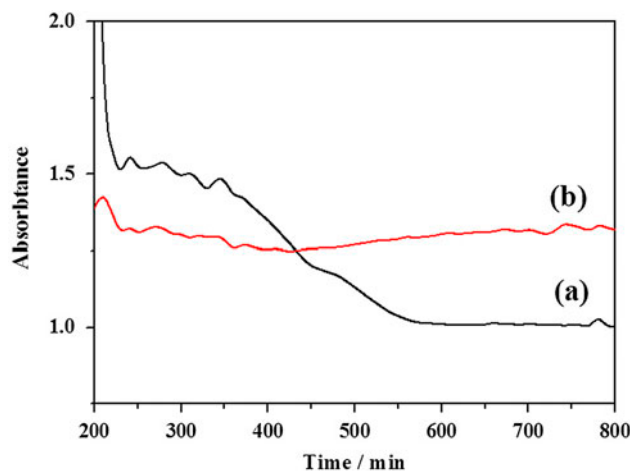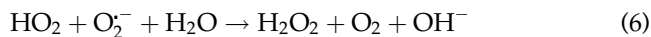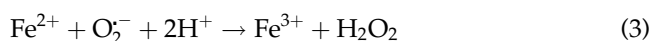
Fig. 12. UV–vis spectra of (a) $Fe^0@PANI$ nanoparticles and (b) after the reaction of $Fe^0@PANI$ nanoparticles in the presence of O_2.

pathway to produce superoxide radicals through Eq. (2), which reacts with ferrous iron or H^+ to form H_2O_2 (Eqs. (2)–(6)) and eventually $\cdot OH$ through the Fenton reaction (Eq. (7)) [33]. Hydroxyl radicals generated can react with target organic contaminants and lead to the mineralization of some organic compounds by converting to CO_2, H_2O, and inorganic ions.

$$Fe^0 \rightarrow Fe^{2+} + 2e^- \tag{1}$$

$$Fe^{2+} + O_2 \rightarrow Fe^{3+} + O_2^{\cdot-} \tag{2}$$

$$Fe^{2+} + O_2^{\cdot-} + 2H^+ \rightarrow Fe^{3+} + H_2O_2 \tag{3}$$

$$O_2^{\cdot-} + H^+ \leftrightarrow HO_2^{\cdot} \tag{4}$$

$$HO_2^{\cdot} + HO_2^{\cdot} \rightarrow H_2O_2 + O_2 \tag{5}$$

$$HO_2 + O_2^{\cdot-} + H_2O \rightarrow H_2O_2 + O_2 + OH^- \tag{6}$$

$$Fe^{2+} + H_2O_2 \rightarrow Fe^{3+} + \cdot OH + OH^- \tag{7}$$

In order to investigate the redox behavior of PANI in the oxidation reaction, the degradation reaction of RhB in the presence of O_2 was followed by using UV–vis spectroscopy. Significant spectral change was observed before and after the reaction (Fig. 12). It can be seen that the characteristic polaron band (470 nm) appeared after the reaction, in the meantime, the absorptance increased obviously from 500 to 800 nm which is attributed to the formation of iron oxide. This result indicates that PANI was oxidized and there was strong interaction between PANI and iron oxide. UV–vis absorption at about 250–350 nm disappeared after the reaction, which is assigned to the reduced form of PANI. These results are consistent with previous Amaya's report on poly(2-methoxyaniline-5-sulfonic acid) (PMAS)/gold nanoparticles [34]. The transition between the reduced and oxidized form of PANI may be partly enhanced the electron transfer in the formation of ROS.

Furthermore, PANI can improve the catalytic performance of nZVI by increasing the surface adsorption of organic matters. The organic compounds with a higher tendency to adsorb to the Fe^0 surface may be oxidized more quickly than those with a low affinity for Fe^0 surface [29]. And in that Fenton system, Fe^{3+} was quickly reduced to Fe^{2+} by the addition of AQS which favors the catalytic redox cycling of iron by promoting the $O_2^{\cdot-}$ production and thus accelerate the degradation of RhB.

On the basis of all the above results and discussions, a proposed reaction mechanism for the aerobic catalytic degradation of RhB over $Fe^0@PANI$ in the presence of AQS is proposed in Fig. 13.

3.4. Stability of $Fe^0@PANI$

It is known that the stability of the catalyst is crucial for its practical application. After each reaction, the catalyst was recovered from the reaction mixture by centrifugation and washed with deionized water and ethanol several times to remove any organic component adsorbed on the surface. As can be seen from Fig. 14, the activity of the catalyst dropped slightly compared with the fresh catalyst. After three times of recycle, the removal efficiency of RhB still reached 82.7% in 120 min reaction. The reduced removal efficiency might be caused by the following reasons: (1) the conglomeration of core-shell
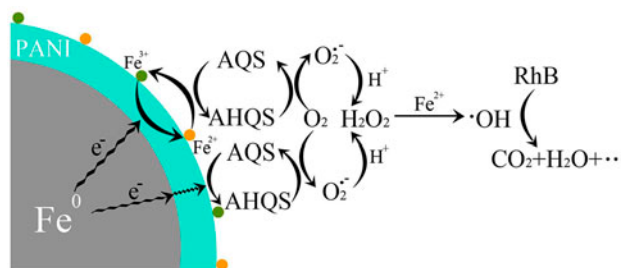

Fig. 13. Proposed reaction mechanism in the degradation of RhB (AQS: anthraquinone-2-sulfonic acid; AHQS: anthrahydroquinone-2-sulfonic acid).
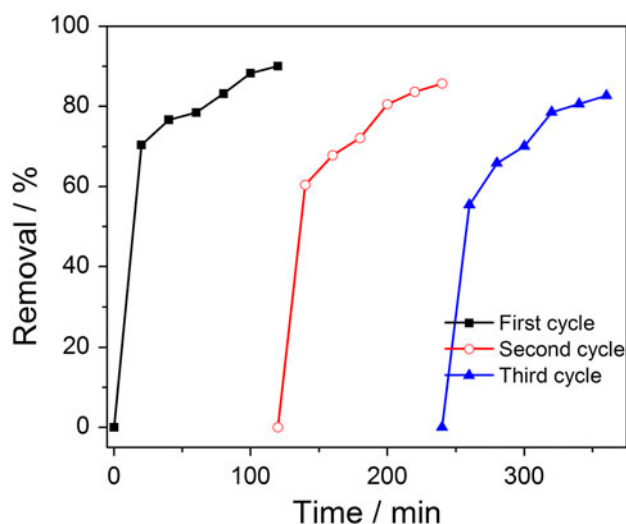
Fig. 14. Different regeneration times on the degradation of RhB (Fe^0@PANI, 0.02 g; AQS, 100 mg/L; initial concentration of RhB, 0.005 mmol/L; pH 6.57).

Fe^0@PANI in some degree led to decrease of activation; (2) the adsorbed fraction of organic contaminants on the surface of nanoparticles inhibited the interaction of core-shell Fe^0@PANI and O_2. Therefore, the good catalytic efficiency, less leached ion species, the long-term stability of core-shell Fe^0@PANI, and convenient recycling without any regeneration made the catalyst attractive.

4. Conclusions

In this study, core-shell Fe^0@PANI nanoparticles characterized by FTIR and XRD have been successfully prepared and were recognized as the efficient and environmental benign nanocatalysts for the treatment of dyeing wastewater. The addition of AQS in Fe^0@PANI/O_2 system increased the oxidation efficiency of RhB, which was ascribed to their role as an electron shuttle. The effect of some operational parameters on the degradation of RhB was investigated. It was found that the degradation efficiency was dependent on pH value, Fe^0@PANI dosage, and initial concentration of RhB. The quenching studies confirmed that hydroxyl radicals were the dominating active species generated in Fe^0@PANI/O_2 process even though at alkaline conditions. Fe^0@PANI exhibited good stability in the Fe^0@PANI/O_2 combined system. The degradation efficiency of RhB was still over 82.7% within 120 min when Fe^0@PANI was used for the third time. Therefore, the proposed method has great potential in the degradation of printing and dyeing wastewater and other refractory organic toxic pollutants.

References

[1] Z.Q. Shi, J.T. Nurmi, P.G. Tratnyek, Effects of nano zero-valent iron on oxidation−reduction potential, Environ. Sci. Technol. 45 (2011) 1586–1592.
[2] H. Song, E.R. Carraway, Reduction of chlorinated ethanes by nanosized zero-valent iron: Kinetics, pathways, and effects of reaction conditions, Environ. Sci. Technol. 39 (2005) 6237–6245.
[3] R.F. Yu, H.W. Chen, W.P. Cheng, Y.J. Lin, C.L. Huang, Monitoring of ORP, pH and DO in heterogeneous Fenton oxidation using nZVI as a catalyst for the treatment of azo-dye textile wastewater, J. Taiwan Inst. Chem. Eng. 45 (2014) 947–954.
[4] W.X. Zhang, Nanoscale iron for environmental remediation: An overview, J. Nanopart. Res. 5 (2003) 323–332.
[5] Y.P. Sun, X.Q. Li, W.X. Zhang, H.P. Wang, A method for the preparation of stable dispersion of zero-valent iron nanoparticles, Colloids Surf., A 308 (2007) 60–66.
[6] Y.Y. Xie, Z.Q. Fang, X.H. Qiu, Comparisons of the reactivity, reusability and stability of four different zero-valent iron-based nanoparticles, Chemosphere. 108 (2014) 433–436.
[7] S. Bleyl, F.D. Kopinke, K. Mackenzie, Carbo-Iron®—synthesis and stabilization of Fe(0)-doped colloidal activated carbon for *in situ* groundwater treatment, Chem. Eng. J. 191 (2012) 588–595.
[8] K. Mackenzie, S. Bleyl, A. Georgi, F.D. Kopinke, Carbo-Iron-An Fe/AC composite-as alternative to nano-iron for groundwater treatment, Water Res. 46 (2012) 3817–3826.
[9] Y. Geng, J. Li, Z. Sun, X. Jing, F. Wang, Polymerization of aniline in an aqueous system containing organic solvents, Synth. Met. 96 (1998) 1–6.
[10] I. Dror, O.M. Jacov, A. Cortis, B. Berkowitz, Catalytic transformation of persistent contaminants using a new composite material based on nanosized zero-valent iron, ACS. Appl. Mater. Interfaces. 4 (2012) 3416–3423.
[11] P. Alexander, O. Nikolay, K. Alexander, Some aspects of preparation methods and properties of polyaniline blends and composites with organic polymers, Prog. Polym. Sci. 28 (2003) 1701–1753.
[12] S. Tsutomu, E.N. Eric, L.C. Edward, A.A. Williama, A polymer membrane containing Fe^0 as a contaminant barrier, Environ. Sci. Technol. 38 (2004) 2264–2270.
[13] T.A. Khan, S. Sharma, I. Ali, Adsorption of Rhodamine B dye from aqueous solution onto acid activated mango (Magnifera indica) leaf powder: Equilibrium, kinetic and thermodynamic studies, J. Toxicol. Environ. Health Sci. 3 (2011) 286–297.
[14] T.A. Khan, M. Nazir, E.A. Khan, Adsorptive removal of Rhodamine B from textile wastewater using water chestnut (Trapa natans L.) peel: Adsorption dynamics and kinetic studies, Toxicol. Environ. Chem. 95 (2013) 919–931.

[15] C. Lee, C.R. Keenan, D.L. Sedlak, Polyoxometalate-enhanced oxidation of organic compounds by nanoparticulate zero-valent iron and ferrous ion in the presence of oxygen, Environ. Sci. Technol. 42 (2008) 4921–4926.

[16] R.A. Doong, H.C. Chiang, Transformation of carbon tetrachloride by thiol reductants in the presence of quinone compounds, Environ. Sci. Technol. 39 (2005) 7460–7468.

[17] F. Aulenta, V.D. Maio, T. Ferri, M. Majone, The humic acid analogue antraquinone-2,6-disulfonate (AQDS) serves as an electron shuttle in the electricity-driven microbial dechlorination of trichloroethene to cis-dichloroethene, Bioresour. Technol. 101 (2010) 9728–9733.

[18] Y.Q. Leng, W.L. Guo, X. Shi, Degradation of Rhodamine B by persulfate activated with Fe_3O_4: Effect of polyhydroquinone serving as an electron shuttle, Chem. Eng. J. 240 (2014) 338–343.

[19] X.S. Lv, J. Xu, G.M. Jiang, X.H. Xu, Removal of chromium(VI) from wastewater by nanoscale zero-valent iron particles supported on multiwalled carbon nanotubes, Chemosphere. 85 (2011) 1204–1209.

[20] D. Li, J. Huang, R.B. Kaner, Polyaniline nanofibers: A unique polymer nanostruc-ture for versatile applications, Acc. Chem. Res. 42 (2009) 135–145.

[21] Q. Wang, S. Snyder, J. Kim, H. Choi, Aqueous ethanol modified nanoscale zerova-lent iron in bromate reduction: Synthesis, characterization, and reactivity, Environ. Sci. Technol. 43 (2009) 3292–3299.

[22] J. Su, S. Lin, Z. Chen, M. Megharaj, R. Naidu, Dechlorination of p-chlorophenol from aqueous solution using bentonite supported Fe/Pd nanoparticles: Synthesis, characterization and kinetics, Desalination. 280 (2011) 167–173.

[23] J. Zhou, S. Yang, J. Yu, Z. Shu, Novel hollow microspheres of hierarchical zinc-aluminum layered double hydroxides and their enhanced adsorption capacity for phosphate in water, J. Hazard. Mater. 192 (2011) 1114–1121.

[24] V.R. Pereira, A.M. Isloor, U.K. Bhat, A.F. Ismail, Preparation and antifouling properties of PVDF ultra-filtration membranes with polyaniline (PANI) nanofi-bers and hydrolysed PSMA (H-PSMA) as additives, Desalination. 351 (2014) 220–227.

[25] S.S. Azim, S. Sathiyanarayanan, G. Venkatachari, Anti-corrosive properties of PANI-ATMP polymer containing organic coating, Prog. Org. Coat. 56 (2006) 154–158.

[26] X. Li, W. Zhang, Iron nanoparticles: The core-shell structure and unique properties for Ni(II) sequestration, Langmuir. 22 (2006) 4638–4642.

[27] X.Q. Li, D.W. Elliott, W.X. Zhang, Zero-valent iron nanoparticles for abatement of environmental pollutants: Materials and engineering aspects, Crit. Rev. Solid State Mater. Sci. 31 (2006) 111–122.

[28] P.G. Tratnyek, M.M. Scherer, B.L. Deng, S.D. Hu, Effects of natural organic matter, anthropogenic surfactants, and model quinones on the reduction of contaminants by zero-valent iron, Water Res. 35 (2001) 4435–4443.

[29] C.R. Keenan, D.L. Sedlak, Factors affecting the yield of oxidants from the reaction of nanoparticulate zero-valent iron and oxygen, Environ. Sci. Technol. 42 (2008) 1262–1267.

[30] S. Song, M. Xia, Z.Q. He, H.P. Ying, B.S. Lü, J.M. Chen, Degradation of p-nitrotoluene in aqueous solution by ozonation combined with sonolysis, J. Hazard. Mater. 144 (2007) 532–537.

[31] A.E. Harvey, J.A. Smart, E.S. Amis, Simultaneous spectrophotometric determination of Iron(II) and total iron with 1,10-phenanthroline, Anal. Chem. 27 (1955) 26–29.

[32] G. Zhang, Y. Gao, Y. Zhang, Y. Guo, Fe_2O_3-pillared rectorite as an efficient and stable fenton-like heterogeneous catalyst for photodegradation of organic contaminants, Environ. Sci. Technol. 44 (2010) 6384–6389.

[33] F.F. Hao, W.L. Guo, X. Lin, Y.Q. Leng, A.Q. Wang, X.X. Yue, L.G. Yan, Degradation of acid orange 7 in aqueous solution by dioxygen activation in a pyrite/H_2O/O_2 system, Environ. Sci. Pollut. Res. 21(2014) 6723–6728.

[34] T. Amaya, T. Ito, Y. Inada, D. Saio, T. Hirao, Gold nanoparticles catalyst with redox-active poly(aniline sulfonic acid): Application in aerobic dehydrogenative oxidation of cyclic amines in aqueous solution, Tetrahedron Lett. 53 (2012) 6144–6147.